Non-linear instability at large vertical displacements in the MAST Tokamak

MJ Windridge[1], G Cunningham[2], TC Hender[2], R Khayrutdinov[3] and V Lukash[4]

[1] Imperial College, London, UK; [2] EURATOM/CCFE Fusion Association, Abingdon, OX14 3DB, UK; [3] TRINITI, Moscow Region, Russia; [4] RRC Kurchatov, Moscow, Russia.

E-mail: `melanie.windridge05@imperial.ac.uk`

Abstract. Data from forced Vertical Displacement Event (VDE) experiments in the Mega Ampère Spherical Tokamak (MAST) indicate that the plasma is highly destabilised above z displacements of $\sim$0.4m. Previous work investigating the plasma response to vertical plasma perturbations in MAST had found it to be more non-linear than an equivalent conventionally-shaped tokamak. Further investigation into the stability of the plasma at high z displacements is done using a linear vertical stability code. Theoretically it is found that the plasma becomes ideally unstable from $z \sim 0.8$m, corresponding to a significant acceleration of the vertical position experimentally.

1. Introduction

It is important to understand the plasma response to vertical displacements in tokamaks, particularly if it is highly non-linear, as this has implications for controller design. Good feedback control is essential to retain the plasma in a stable equilibrium and minimise the likelihood of Vertical Displacement Events (VDEs)[1]. A VDE is the vertical movement of the plasma (upwards or downwards) culminating in a disruption when the feedback system fails to retain the plasma in the desired position[2]. The major consequences of VDEs are heat loads to the wall and electromagnetic forces that are generated as a result of both induced currents and currents that flow from the plasma into the vacuum vessel when the plasma makes contact, termed halo currents[3][4].

The design of the Mega Ampère Spherical Tokamak (MAST) is quite different to other tokamaks, both spherical and conventional. The MAST vessel is large and cylindrical and, unusually, has poloidal field (PF) coils internal to the vessel[5]. This arrangement gives increased flexibility and greater diagnostic accessibility, but does mean that the stability advantage of a close-fitting shell is lost. MAST, as a spherical tokamak, has naturally higher-elongation plasmas and thus increased vertical stability at a given elongation and plasma inductance compared to a conventional aspect ratio tokamak[6]. Despite this, previous work has identified the response of the MAST plasma to vertical displacements to be more non-linear than for an equivalent conventional

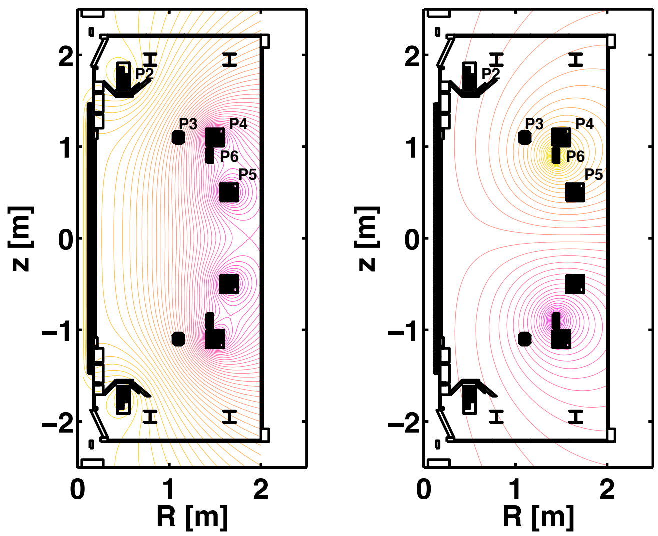

Figure 1. The typical MAST vacuum field (left) and the field from the P6 coil (right). At high z excursions the curvature of the vacuum field greatly increases, which will have a destabilising effect on the plasma. At this height the radial feedback field from the P6 coil used to stabilise the plasma becomes ineffectual as the plasma is in a region where the radial field is minimal. Note the lack of a close-fitting, stabilising wall. In MAST, passive stabilisation is provided predominantly by the casings surrounding the PF coils.

tokamak[7]. This is due to the combination of the inhomogeneity of the vertical field and the reduction in efficacy of the vertical control system with increasing z displacement (at high displacements there is a loss of radial field to provide this control). All these features of MAST can be seen in Figure 1. This paper looks at experiment and theory to determine that these features act together in MAST to create high vertical instability at large displacements.

2. Plasma stability at high z displacements in MAST experiment

Whilst studying triggered VDEs in MAST, it was found that the plasma vertical instability growth rate increased rapidly with increasing z displacement. The VDEs were triggered by cutting the feedback stabilisation and the plasma was positioned a few centimetres above the midplane to encourage an immediate response. Centre column vertical field (CCBV) measurements and soft X-ray data were used to derive measurements of z excursion.

The centre column B_v array consists of 2 sets of 40 B_v Mirnov coils positioned under the centre column graphite armour, the 2 sets 180° apart toroidally, which measure the vertical field from $z = \pm 1.5$m. The peak of the CCBV signals is found where $dB_v/dz = 0$ and the corresponding z is taken as the vertical position of the plasma. Figure 2 shows X-ray data from a selection of chords across the plasma along with a cross-section of the MAST vacuum vessel giving the views of these chords through the plasma. These

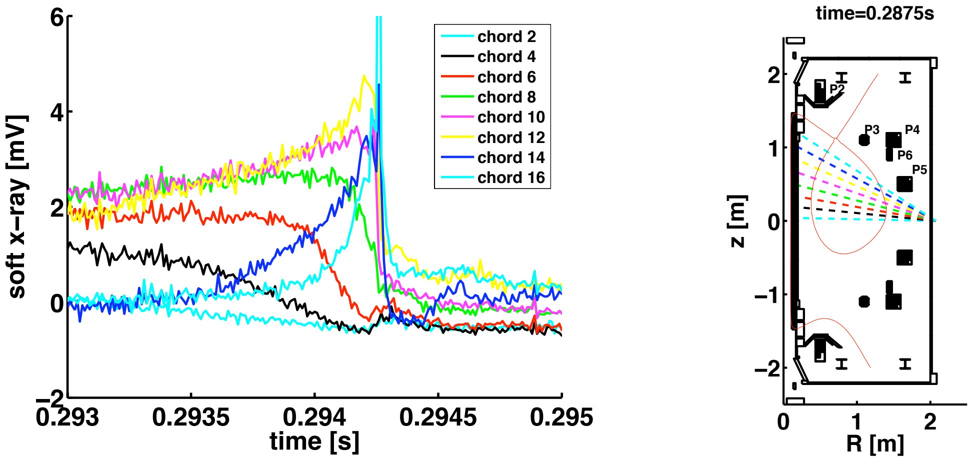

Figure 2. Left: soft X-ray data from a selection of chords for shot 19697 during the VDE. Right: a cross-section of the MAST vacuum vessel with the view of the lower soft X-ray camera showing the selected chords. The legend applies to both plots.

line-integral values of X-ray emissivity were used along with the height of the chords to calculate an approximation for the z excursion of the plasma as follows:

$$z(t) = \frac{\sum_{chords}(I(t) \times z_{chord})}{\sum_{chords} I(t)} \tag{1}$$

where $I(t)$ is the intensity of the soft X-ray emissivity and z_{chord} is the height of the chord on the centre column. Both sets of z data were compared with equilibrium reconstructions from the EFIT[8] code from early in the shot and any necessary adjustments were made for offsets of the signals. A comparison of each dataset with EFIT is shown in Figure 3, and Figure 4 shows that the z evolution calculated from the CCBV and soft X-ray data correlate very well.

Figure 5 shows how the vertical instability growth rate changes throughout the VDE. The left-hand plot shows best-fit lines used to approximate the gradient at intervals. After the feedback is cut at 0.25s up to 0.28s, the growth rate is approximately constant at 40s^{-1}. Between 0.28s ($z = 0.11$m) and 0.29s ($z = 0.25$m) the growth rate increases to approximately 82s^{-1}, but then after 0.29s the plasma begins to accelerate rapidly and by 0.2936s the growth rate is approaching 2000s^{-1}. This time corresponds to a position of $z = 0.44$m. The right-hand plot shows the vertical instability growth rate γ calculated as the derivative of $log(z)$ and smoothed separately over the intervals 0.24-0.28s, 0.28-0.29s and 0.29-0.293s. Data from $t > 0.293$s is not smoothed and shows the full extent of the increase in growth rate after 0.293s. The maximum vertical instability growth rate is shown to be $\sim$1800s^{-1}.

The plasma is clearly greatly destabilised by this point, though the vertical instability growth is still slow compared to Alvénic timescales. The toroidal magnetic field at the plasma axis is taken as $B_0 = 0.5$T, the minor radius $a = 0.5$m and the mass density is $\rho_0 = 3.34 \times 10^{-8}$kgm^{-3} (corresponding to an electron number density of $n_e = 10^{19}$m^{-3}) giving an inverse Alfvén time of 5×10^6s^{-1}.

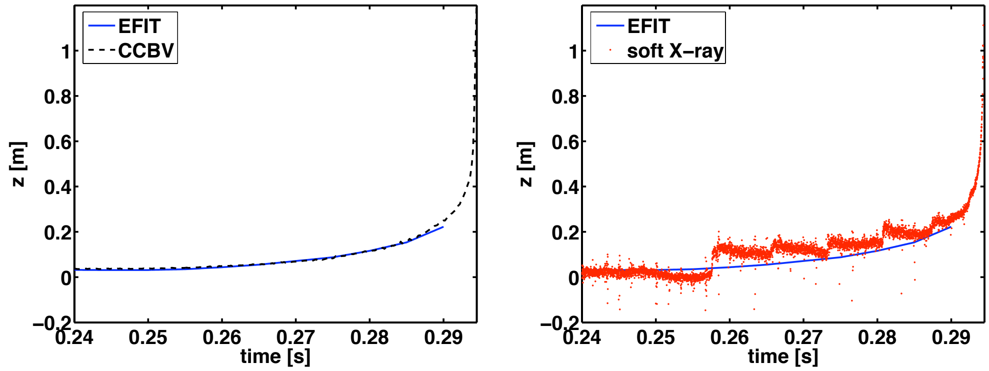

Figure 3. The plasma z position from EFIT (solid line) compared with the z position calculated from the CCBV data (left) and the soft X-ray data (right). Shot 19697.

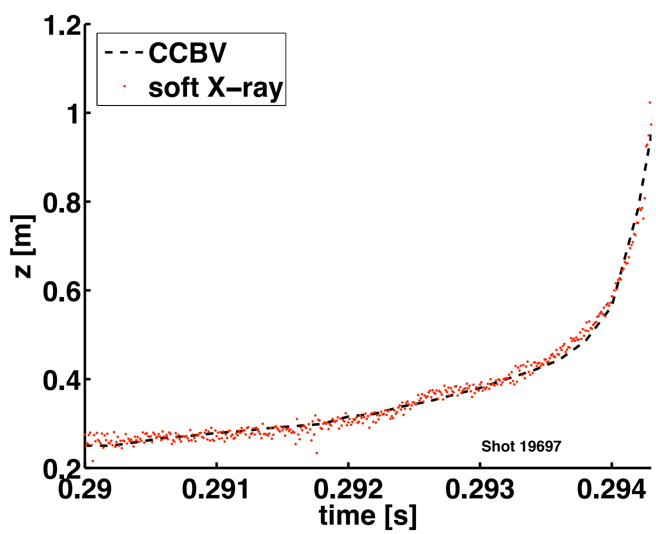

Figure 4. The CCBV and soft X-ray data in the time just preceding the thermal quench, when EFIT data is no longer available. Shot 19697.

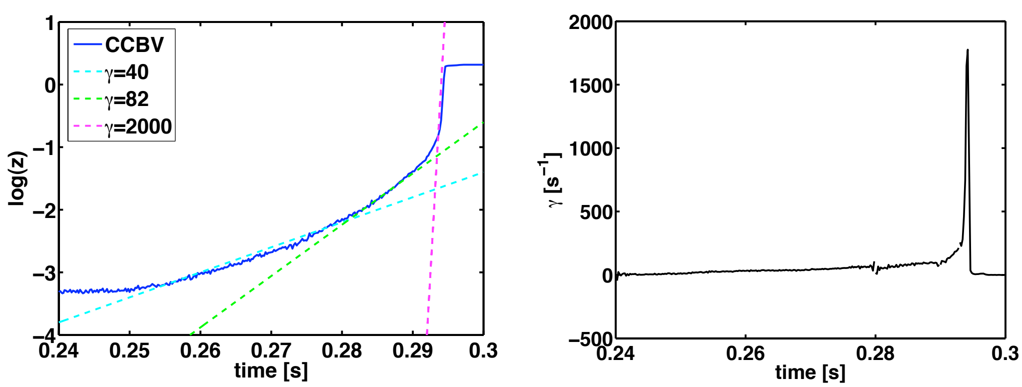

Figure 5. Left: Log of the CCBV z signal showing how the vertical instability growth rate of the plasma changes throughout the VDE. After t=0.29s this rate changes considerably. Right: How the vertical instability growth rate changes with time. Shot 19697.

In MAST, passive stabilisation is provided predominantly by the casings surrounding the PF coils P3 and P6, as these coils are in the most stabilising position (just outside the plasma on a poloidal angle of around 70°) as demonstrated by Leuer[9]. Knowing the non-linearity in the MAST passive stabilising field structure (similar to Figure 1, right-hand plot) at high z displacements, it is proposed that the MAST plasma reaches an excursion at which the passive stabilisation is no longer sufficient to balance the destabilising force on the plasma, ie. it becomes ideally unstable with the vertical instability growth rate determined by the plasma inertia.

3. Theoretical investigation of plasma stability in MAST at high z displacements

Having seen the unusually high vertical instability growth rate of high z displacement MAST plasmas, the stability of the MAST plasma was examined using a free-boundary plasma equilibrium code—Fiesta—and the RZIP[10] linearised stability model. An attempt was also made to simulate the VDEs with the tokamak simulation code DINA-CH[11][12]. DINA was unable to track the z growth in MAST at high vertical displacements, despite a good record of VDE tracking and halo current simulation in other tokamaks. Beyond $z \sim 0.5$m the plasma was too unstable and jumped to the top of the vessel in one timestep. However, using Fiesta and RZIP it was possible to calculate the variation in the parameter f_s, which gives a measure of the stability of the plasma.

The parameter f_s, defined by Leuer[9], is the ratio of the stabilising to the destabilising force gradient in z.

$$f_s = -\frac{F_s'}{F_d'} \tag{2}$$

where subscripts s and d represent stabilising and destabilising forces on the plasma respectively, the prime represents differentiation with respect to z. The stabilising term F_s' is the force gradient on the plasma due to eddy currents flowing in the passive structure generated by the movement of the plasma. The destabilising term F_d' is the force gradient on the plasma due to the curvature of the external vertical magnetic field (in other words, due to the currents in the PF coils). Thus f_s can be calculated from the set of mutual inductance matrices $\mathbf{M}$ describing the interactions between the plasma, the passive structure and the PF coils as

$$f_s = \frac{\mathbf{I}_p^T \mathbf{M}'_{p,s} \mathbf{M}_{s,s}^{-1} \mathbf{M}'_{s,p} \mathbf{I}_p}{\mathbf{I}_p^T \mathbf{M}''_{p,PF} \mathbf{I}_{PF}} \tag{3}$$

where the subscript p represents plasma, s represents the stabilisation conductors and PF the PF coils. $\mathbf{I}_p^T$ is the transpose of the plasma current vector.

The f_s parameter is often used to determine the suitability of a given passive structure configuration since the value of f_s reflects the controllability of the plasma based on the passive structure characteristics.

$f_s < 0$	means the plasma is stable;
$f_s > 1$	means the plasma is unstable but with the instability growth rate limited by the passive eddy currents, and with f_s getting closer to 1 as the plasma becomes less controllable;
$0 < f_s < 1$	means the plasma is ideally unstable.

If $f_s > 1$ then the vertical instability growth rate of the system is governed by the resistive timescale of the passive structure ($\tau_{passive}$) and the plasma inertia can be neglected. In this case the growth rate can be expressed as

$$\gamma = \frac{1}{\tau_{passive}} \frac{1}{(f_s - 1)}. \tag{4}$$

However, it should be noted here that this expression is valid in the case of a simple passive system with a relatively uniform time constant $\tau_{passive}$, but it is not so appropriate for MAST, whose unique structure makes it impossible to calculate a simple $\tau_{passive}$. It can be seen here that the vertical instability growth rate becomes infinite as f_s approaches unity, which may explain the sharp jump observed in the DINA simulation. For $f_s < 1$ the plasma mass becomes important, the growth rate is dominated by inertial terms and the plasma will move on an Alfvén timescale ($\sim 5 \times 10^6\text{s}^{-1}$ for the case considered here).

To investigate this, Fiesta was used to create equilibria beyond the final EFIT reconstruction time for MAST shot 19697. Fiesta is a free boundary, Grad-Shafranov equilibrium solver, not a full dynamic model, so gives a qualitative description only, but by examining these artificial equilibria we are able to assess the stability of the plasma in regions where experimental data are not available. The initial Fiesta boundary was constructed from EFIT parameters of the last equilibrium it was able to calculate ($t = 0.285$s). From this equilibrium the plasma was slowly moved upwards to specified z values, 0.05m at a time from $z = 0.2 - 0.75$m. This was done by adding a small, uniform radial field to stabilise the z position. Being uniform, this doesn't affect the plasma shape or the RZIP stability calculation. The corresponding equilibrium was calculated using the core plasma current and currents in the PF coils taken from experiment at the time the plasma was at that particular z position, as measured by the centre column vertical field (Mirnov) coils.

Beyond a z position of 0.75m, Fiesta was unable to converge the equilibria as the plasma became limited on the P3 coil. This is thought to be unrealistic—because the shrinking plasma boundary would reduce q_0 too much—and likely due to eddy currents not being included in the Fiesta calculation. In order to notionally represent these eddy currents the vertical magnetic field was increased slightly to push the plasma inwards and away from the P3 coil for the last three equilibria. This is consistent with initial analysis of visible light plasma images. Figure 6 shows the boundaries of the equilibria calculated by Fiesta, the red one being the last of the EFIT data.

From these equilibria Fiesta can then calculate the parameter f_s and the vertical instability growth rate using the RZIP algorithm. The RZIP model represents the

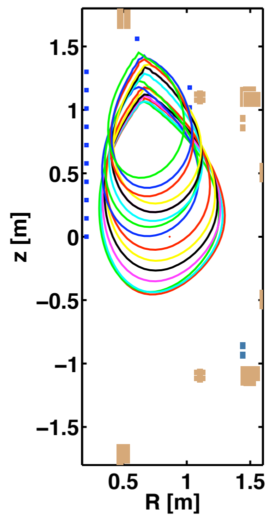

Figure 6. Equilibria calculated by the Fiesta code. The lowest red boundary is taken from EFIT data and the other, higher equilibria were converged by Fiesta and used to calculate the Leuer parameter.

vacuum vessel, PF coils and passive structure as toroidal current carrying filaments. It assumes the plasma current to be distributed over the cross-section of the plasma and the current profile to be independent of movements in R and z. RZIP calculates mutual inductance matrices between this distributed but rigid plasma and all parts of the active and passive structure, and the response of the plasma to control actions (changes in the coil voltages) is reduced to a set of circuit equations as detailed in reference [10]. f_s is calculated by RZIP from these mutual inductance matrices, I_p and the PF coil currents. The effect of eddy currents flowing in the passive structure are included in the calculation, but halo currents are not accounted for. Figure 7 shows how the f_s parameter changes as z increases. For all the Fiesta-generated equilibria up to $z = 0.75$m, ie. those using experimental core I_p and coil currents, the f_s parameter approaches 1, indicating that the plasma is becoming more nearly ideally unstable. Beyond $z = 0.8$m, where the plasma is pushed inwards and higher by Fiesta by the addition of an artificial vertical field, the f_s parameter drops below 1, indicating that the plasma has become ideally unstable.

From this data, we conclude that the large vertical instability growth rate in the MAST experiment is due to the increasing instability of the MAST plasma at high z displacements, as shown by the rapid decrease of the f_s parameter. The "jumping plasma" in DINA is due to the rapidly rising vertical instability growth rate culminating in the plasma becoming ideally unstable at high z. This is a real effect that may

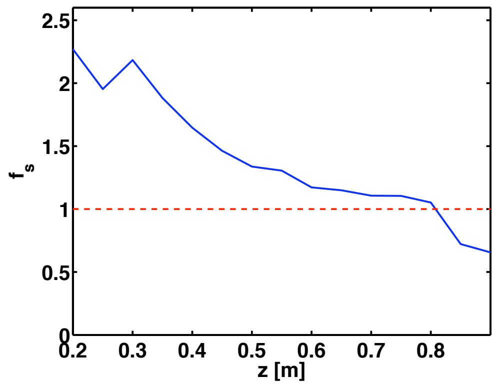

Figure 7. The Leuer parameter f_s plotted against the position of the z axis for each of the equilibria shown in Figure 6. The plasma becomes ideally unstable when the Leuer parameter drops below 1.

be unique to MAST and due to the machine structure, though the vertical instability growth rate seen in the experiment is three orders of magnitude below the Alfvén growth time.

4. Conclusions

MAST plasmas are more vertically unstable at high z displacements than would usually be expected. Examination of the experimental centre column Mirnov coil and soft X-ray data confirms that the plasma is highly destabilised from ∼0.4m. The plasma movement was found to greatly accelerate with increasing z. For MAST shot 19697, the plasma vertical instability growth rate changed from $40s^{-1}$ below 0.1m, through $80s^{-1}$ for excursions up to 0.25m and reached approximately $1800s^{-1}$ by around 0.44m. Theory shows that, for the same shot, the f_s parameter falls below 1 at a z displacement of 0.8m, indicating that the plasma has become ideally unstable.

While STs generally have better vertical stability properties due to higher natural elongation, a unique combination of effects in MAST leads to strong non-linearity of the vertical instability. This is attributable to a combination of distinct features in MAST: the high curvature of the vertical magnetic field at high z; the lack of stabilisation from a close-fitting passive structure; and the progressive loss of the passively-induced radial field to apply a restoring vertical force as the plasma moves further away from equilibrium.

Acknowledgments

This work was funded by the UK Engineering and Physical Sciences Research Council under grant EP/G003955 and by the European Communities under the contract of association between Euratom and CCFE. The views and opinions expressed herein do not necessarily reflect those of the European Commission.

References

[1] Lister JB et al. 1990 *Nuclear Fusion* **30(11)** 2349-2366
[2] ITER Physics Expert Group on Disruptions, Plasma Control and MHD and ITER Physics Basis Editors 1999 *Nuclear Fusion* **39(12)** 2251-2389
[3] Thomas PR et al. 1985 *Plasma Physics and Controlled Nuclear Fusion Research, IAEA, Vienna* **I** 353
[4] Gruber O et al. 1993 *Plasma Phys. Control. Fusion* **35** B191-B204
[5] Sykes A et al. 2001 *Nuclear Fusion* **41(10)** 1423
[6] Sykes A 1994 *Plasma Phys. Control. Fusion* **36** B93
[7] Windridge MJ et al. 2008 *35th EPS Conf. on Plasma Physics and Cont. Fusion (Hersonissos)* 32D(P-4.066)
[8] Lao LL et al 1985 *Nuclear Fusion* **25(11)** 1611-1622
[9] Leuer JA 1989 *Fusion Technology* **15** 489-494
[10] Coutlis A et al. 1999 *Nuclear Fusion* **39(5)** 663-683
[11] Khayrutdinov RR and Lukash VE 1993 *J. Comput. Phys.* **109(2)** 193-201
[12] Khayrutdinov RR et al. 2003 *30th EPS Conf. on Plasma Physics and Cont. Fusion (St Petersburg)* 27A(P-3.163)